

FPGA-based adaptive noise cancellation for ultrasonic NDE application

Christopher Brady, Jessica Arbona, In Soo Ahn and Yufeng Lu*

Department of Electrical and Computer Engineering
Bradley University, Peoria, Illinois 61625

Abstract— Adaptive filter has been widely used in different applications for interference cancellation, predication, inverse modeling and identifications. In this paper, Field Programmable Gate Array (FPGA)-based adaptive noise cancellation is studied for adaptive filtering in ultrasonic non-destructive evaluation. Simulation and experimental results showed that backscattered noise from microstructures inside material can be efficiently reduced by adaptive filter. Additionally, four different architectures of filter realization on FPGA are discussed and compared. This type of study could have a broad range of applications such as target detection, object localization and pattern recognition.

Keywords- *FPGA, non-destructive evaluation, adaptive filter, ultrasonic backscattered signal;*

I. INTRODUCTION

In radar, sonar, medical ultrasound, and industrial ultrasonic applications, the detected signal always contains backscattered echoes from ground, sea, scatters, or microstructures inside material [1-4]. These echoes are high overlapped and greatly dependent on the complex physical properties of the propagation path. It is challenging to extract valuable information from detected signals especially in the applications of target localization, flaw detection, object recognition, etc.

In ultrasonic nondestructive evaluation (NDE), the backscattered noise is primarily from crystallites (i.e., grains). They have irregular boundaries, size and random orientation. The signal representation of flaw or defect may be not identified due to the high density scattering grains. Much research effort has been made to suppress grain noise and process ultrasonic data. Split spectrum processing (SSP), discrete wavelet transform (DWT), discrete Hadamard transform (DHT), discrete cosine transform (DCT), and chirplet transform have been utilized for ultrasonic signal processing [5-11]. Additionally, nonlinear order statistical filter, neural network, and morphological processing have been explored [12-15]. It can be seen that a signal processing technique adaptive to ultrasonic data is highly sought-after.

Adaptive filter is widely used in different applications for interference cancellation, prediction, inverse modeling, and identification. Nevertheless, there is no much discussion done in ultrasonic backscattered signal analysis.

Least mean square (LMS) and recursive least square (RLS) are commonly adopted to implement adaptive filters [16-17]. In [18], normalized LMS is explored for ultrasonic backscattered signal. In [19-20], ultrasonic NDE signals and medical ultrasound images are deconvoluted using adaptive filter. In [21], a simulation study of adaptive filter on ultrasonic NDE signals has been conducted. Normalized least mean square (NLMS) and recursive least square (RLS) algorithms have been applied to ultrasonic data. In this paper, FPGA-based adaptive noise cancellation is studied for ultrasonic NDE application. Different realization structures of adaptive filter are discussed and compared. This type of work could have a broad range of applications especially for hardware realization of real-time adaptive filtering.

This paper is organized as follows: Section II briefly reviews adaptive filter, especially NLMS for ultrasonic signal processing. Section III discusses the design consideration of FPGA-based adaptive noise cancellation system and covers different filter realization structures. Section IV shows software simulation and hardware implementation results. Section V concludes the paper.

II. ADAPTIVE FILTERING FOR ULTRASONIC SIGNAL

In the adaptive filter (see Figure 1), $d(n)$ denotes a primary input of the system, $x(n)$ the adaptive filter input signal, $y(n)$ the adaptive filter output signal, and the error signal, $e(n)$, is the difference between $d(n)$ and $y(n)$.

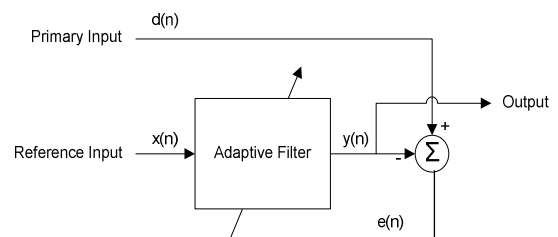


Figure 1. General block diagram of adaptive filtering system

The filter output, $y(n)$, can be written as

$$y(n) = \sum_{i=0}^{L-1} w_i(n) x(n-i) = W^T(n)X(n) \quad (1)$$

where the vector $W(n) = [w_0(n) \ w_1(n) \ \dots \ w_{L-1}(n)]^T$ denotes the coefficients of the time-varying L-tap adaptive filter, $X(n) = [x(n) \ x(n-1) \ \dots \ x(n-L+1)]^T$ denotes the filter input vector, and $[\bullet]^T$ denotes the transpose operation.

The filter coefficients, $W(n)$, are adjusted to minimize the mean square error function of the system, $J(n)$, given by

$$\begin{aligned} J(n) &= E[e^2(n)] \\ &= E[d^2(n)] - W^T(n)E[X(n)d(n)] \\ &\quad - E[d(n)X^T(n)]W(n) + W^T(n)E[X(n)X^T(n)]W(n) \\ &= E[d^2(n)] - 2W^T(n)r_{dx}(n) + W^T(n)R_{xx}(n)W(n) \end{aligned} \quad (2)$$

where auto correlation matrix is defined by $R_{xx}(n) = E[X(n)X^T(n)]$, cross correlation matrix $r_{dx}(n) = E[X(n)d(n)]$.

To do so, the partial derivative of $J(n)$ with respect to the filter coefficients, $W(n)$ is set to zero.

$$\frac{\partial J(n)}{\partial W^T(n)} = 0 \quad (3)$$

The solution of equation (3) can be written as

$$W_{opt}(n) = R_{xx}^{-1}(n)r_{dx}(n) \quad (4)$$

The computation cost of equation (4) is enormous due to the matrix inversion calculation for every new data sample. Therefore, an iterative strategy is commonly used to update the filter coefficients, $W(n)$.

NLMS is one of typical algorithm used in adaptive filter.

The filter coefficients vector is updated as [17-18]

$$W(n+1) = W(n) + \eta e(n)X(n) \quad (5)$$

where η is the learning factor to control the convergence rate of the filter. It can be updated as

$$\eta = \frac{2}{\delta + p(n)} \quad (6)$$

where δ is a small value to limit the learning rate and $p(n)$ is the estimated signal power. $p(n)$ is updated by

$$p(n) = \zeta p(n-1) + x^2(n) \quad (7)$$

where ζ is the forgetting factor of $p(n)$.

In adaptive noise cancellation, the primary input, $d(n)$, and the reference input, $x(n)$, can be defined as

$$\begin{aligned} d(n) &= s(n) + g_1(n) \\ x(n) &= g_2(n) \end{aligned} \quad (8)$$

where $d(n)$ is the signal contaminated by a noise, $g_1(n)$; $g_2(n)$ is a referenced noise input.

In noise cancellation, the referenced noise signal, $g_2(n)$, is always available for the system. In ultrasonic application, the grain noise is strongly related to the position of the transducer. In another word, it is difficult to separate the flaw echo from the grain echoes and obtain a clean reference grain signal for adaptive filter. Therefore, ultrasonic data including correlated flaw echo and different level of grain noise are used for adaptive filtering.

An ultrasonic data acquisition system is setup to acquire experimental backscattered data using a 5MHz transducer and 100 MHz sampling rate. The specimen is a steel block with a flat-bottom hole (i.e., target). NLMS adaptive filter has been used to process the acquired ultrasonic data [18, 21]. The simulation result of a 6-tap filter is shown in Figure 2.

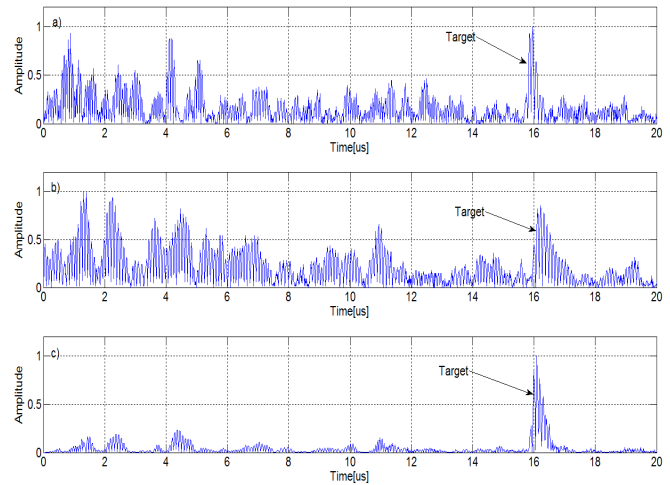


Figure 2 a) The primary input : ultrasonic experimental signal. b) The reference input to the adaptive filter: ultrasonic signal. c) The output signal from the adaptive filter.

It can be seen that NLMS adaptive filter greatly improves the signal-to-grain noise ratio by around 12 dB (Figure 2c) and detect the target successfully

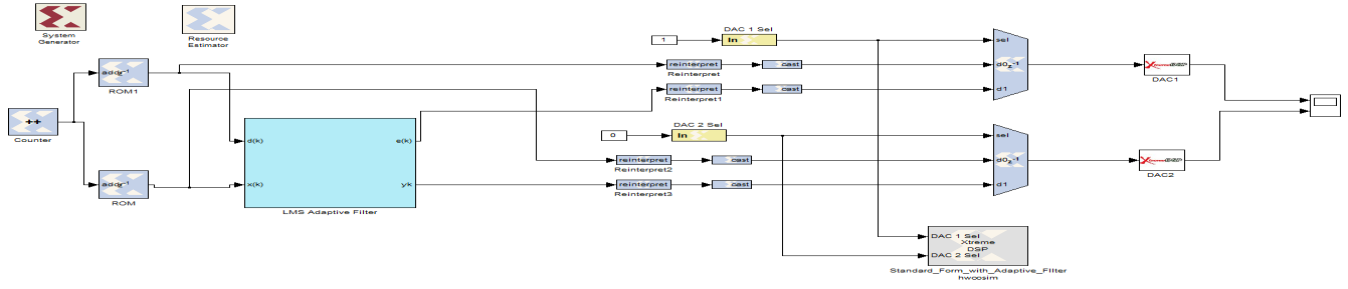


Figure 3. Adaptive noise cancellation using Xilinx system generator.

III. FPGA-BASED ADAPTIVE NOISE CANCELLATION

Field Programmable Gate Array (FPGA) has been widely used in applications such as communication, industrial automation, motor control, medical imaging etc. It is reconfigurable in term of digital logic, input/output block, and routing resource. In addition, algorithms running on FPGA could have a real-time performance with signal processing in parallel on hardware. Instead of using conventional hardware Description language, Xilinx system generator is used to implement the adaptive noise cancellation system. Thanks to model-based design environment of MATLAB/Simulink and predefined block sets of DSP cores, the system generator is used to prototype a signal processing system rapidly on an extremeDSP Virtex 4 FPGA board. Figure 3 illustrates the block diagram of adaptive noise cancellation. It includes two ROMs to hold ultrasonic data, two multiplexers and DACs to probe internal signals, an hwcosim block to perform hardware-in-loop verification and an NLS adaptive filter. The adaptive filter realization (see Figure 4) mainly includes two parts: fixed-point FIR filter realization and coefficient update.

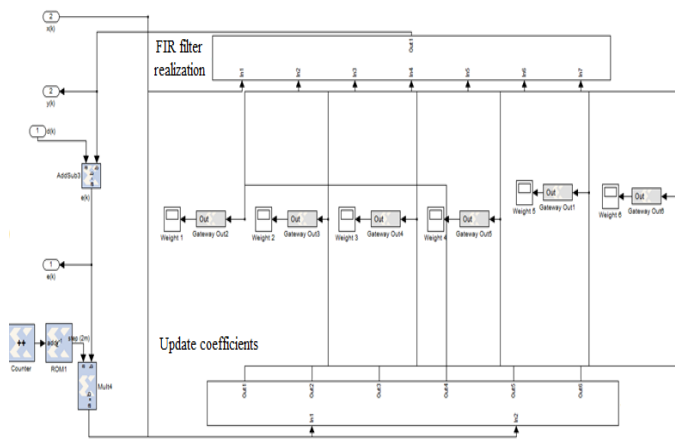


Figure 4. Block diagram of adaptive filter realization

The standard realization structure of 6-tap FIR filter (see equation 1) is shown in Figure 5. Simulation results from the fixed-point standard FIR realization and the floating-point MATLAB are shown in Figure 6.

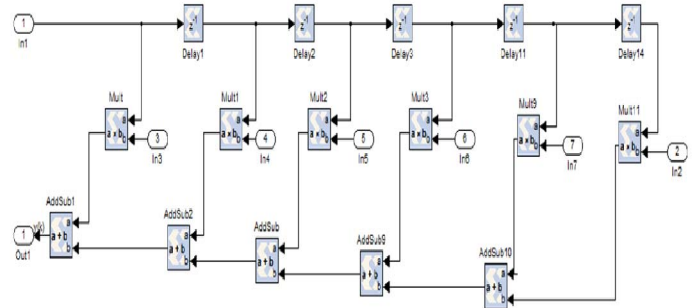


Figure 5. Standard FIR realization structure

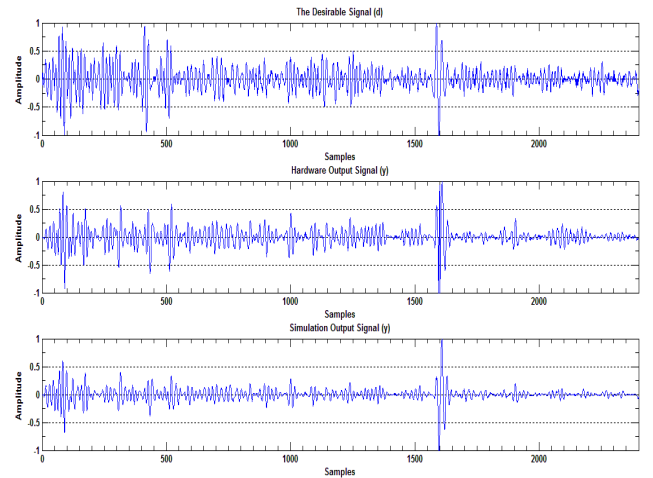


Figure 6. a) Ultrasonic experimental data for the input of adaptive filter. b) The simulation result of standard fixed-point FIR realization c) The simulation result from MATLAB

The critical path (i.e., the longest propagation delay), τ_1 , for standard FIR form can be written as

$$\tau_1 = \tau_{mult} + 5 \tau_{add} \quad (9)$$

where τ_{mult} denotes the delay of multiplier
 τ_{add} denotes the delay of adder

To improve the FIR performance, especially the speed of adaptive filter, a systolic FIR realization structure is evaluated (see Figure 7). The corresponding simulation results are shown in Figure 8. It can be seen the critical path is greatly reduced to $\tau_{mult} + \tau_{add}$.

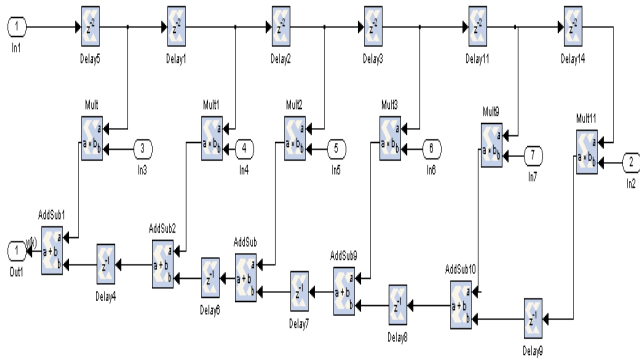


Figure 7. Systolic FIR realization structure

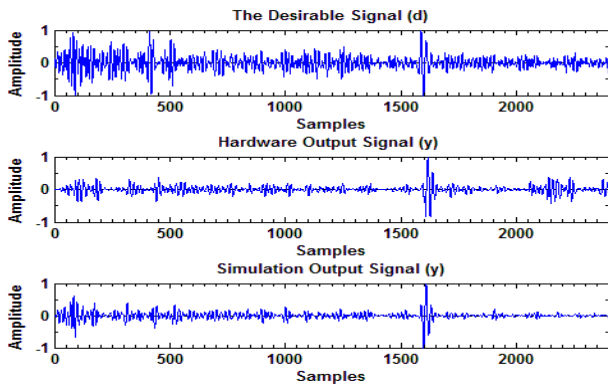


Figure 8. a) Ultrasonic experimental data for the input of adaptive filter. b) The simulation result of fixed-point systolic FIR realization c) The simulation result from MATLAB

To further improve the speed and throughput of adaptive filter, the systolic FIR realization structure is pipelined (see Figure 9). The improved critical path is determined by the bigger value of τ_{mult} and τ_{add} , which can be denoted as $\max(\tau_{mult}, \tau_{add})$. The corresponding simulation results are shown in Figure 10.

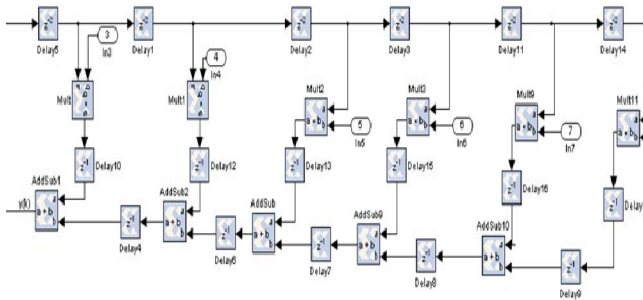


Figure 9. Pipelined systolic FIR realization structure

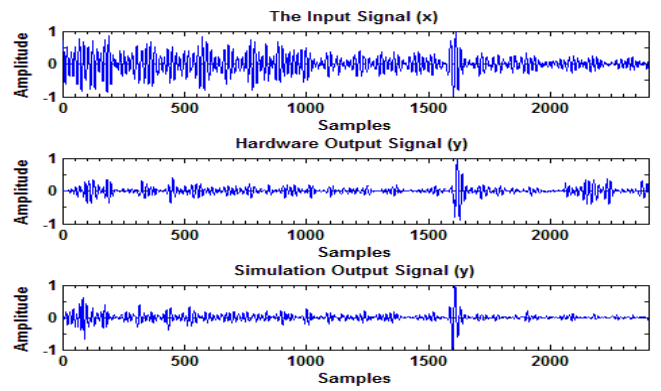


Figure 10. a) Ultrasonic experimental data for the input of adaptive filter. b) The simulation result of fixed-point systolic FIR realization c) The simulation result from MATLAB

From above discussion, it can be seen that adaptive filter can successfully track the flaw signal embedded in ultrasonic backscattered grain echoes by noise cancellation. Three different FIR realization structures are evaluated. The pipelined systolic structure has the best performance in terms of system throughput and speed. It should be mentioned that more resource usage is incurred due to extra logics for pipelined systolic structure. Furthermore, Figure 11 shows hardware implementation result on oscilloscope.

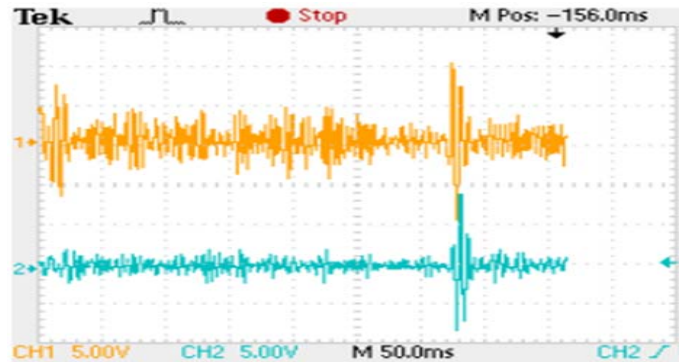


Figure 11. Hardware implementation result on oscilloscope. Top: ultrasonic experimental data for the input of adaptive filter. Bottom: the output of adaptive filter.

IV. CONCLUSION

In this study, adaptive filter has been introduced to analyze ultrasonic backscattered signals. FPGA-based adaptive noise cancellation is designed. Three different filter realization structures have been evaluated and compared. Software simulation and hardware simulation shows that the adaptive filter could be an effective tool for ultrasonic NDE application.

REFERENCES

- [1] H. W. Melief, H. Greidanus, P. Genderen, and P. Hoogeboom, "Analysis of sea spikes in radar sea clutter data", *IEEE Transaction on Geoscience and Remote Sensing*, Vol. 44, no. 4, pp. 985-993, April 2006.

- [2] G.D. De Grandi, J. Lee, and D. L. Schuler, "Target detection and texture segmentation in polarimetric SAR images using a wavelet frame: theoretical aspects", *IEEE Transaction on Geoscience and Remote Sensing*, Vol. 45, no. 11, pp. 3437-3453, November 2007.
- [3] G. Cincotti, G. Loi, and M. Pappalardo, "Frequency decomposition and compounding of ultrasound medical images with wavelet packets", *IEEE Transaction on Medical Imaging*, Vol. 20, pp. 764-771, August 2001.
- [4] Y. Lu, R. Demirli, G. Cardoso, and J. Saniie, "A successive parameter estimation algorithm for chirplet signal decomposition," *IEEE Transaction on Ultrasonics, Ferroelectrics, and Frequency Control*, vol. 53, pp. 2121–2131, November 2006.
- [5] E. Oruklu, and J. Saniie, "Hardware efficient realization of a real time ultrasonic target detection system," *IEEE Transaction on Ultrasonics, Ferroelectrics, and Frequency Control*, vol. 56, no. 6, pp. 1262-1269, June 2009.
- [6] E. Oruklu, and J. Saniie, "Dynamically reconfigurable architecture design for ultrasonic imaging," *IEEE Transaction on Instrumentation and Measurement*, vol. 58, no. 8, pp. 2856-2866, August 2009.
- [7] H. C. Sun, and J. Saniie, "Ultrasonic flaw detection using split-spectrum processing combined with adaptive network based fuzzy inference system," *IEEE Proceedings of Ultrasonic Symposium*, vol.1, pp. 801-804, 1999.
- [8] M. Grevillot, C. Cudel, J. Meyer, and S. Jacquey, "Two approaches to multiple specular echo detection using split spectrum processing: moving bandwidth minimization and mathematical morphology," *Ultrasonics*, vol. 26, pp. 204-209, 1998.
- [9] Y. Lu, E. Oruklu, and J. Saniie, "Fast chirplet transform with FPGA-based implementation," *IEEE Signal Processing Letters*, vol. 15, pp. 577-580, December 2008.
- [10] Y. Lu, R. Demirli, and J. Saniie, "A comparative study of echo estimation techniques for ultrasonic NDE applications," *IEEE Proceedings of Ultrasonic Symposium*, pp. 536–539, October 2006.
- [11] Y. Lu, R. Demirli, G. Cardoso, and J. Saniie, "Chirplet transform for ultrasonic signal analysis and NDE applications," *IEEE Proceedings of Ultrasonic Symposium*, vol. 1, pp. 18-21, September 2005.
- [12] H. C. Sun, and J. Saniie, "Nonlinear signal processing for ultrasonic target detection," *IEEE Proceedings of Ultrasonic Symposium*, vol.1, pp. 855-858, 1998.
- [13] S. Yoon, E. Oruklu, and J. Saniie, "Dynamically reconfigurable neural network hardware design for ultrasonic target detection," *IEEE Proceedings of Ultrasonic Symposium*, pp. 1377-1380, 2006.
- [14] M. A. Mohamed, and J. Saniie, "Ultrasonic flaw detection based on mathematical morphology," *IEEE Transaction on Ultrasonics, Ferroelectrics and Frequency Control*, vol. 41, no.1, pp. 150-160, 1994.
- [15] M. A. Mohamed, and J. Saniie, "Statistical evaluation of sequential morphological operations," *IEEE Transaction on Signal Processing*, vol. 43, no.7, pp. 1730-1709, 1995.
- [16] A. H. Sayed, "*Fundamentals of adaptive filtering*," Wiley – Interscience, John Wiley & Sons, Inc. , 2003.
- [17] U. M. Baese, "Digital signal processing with field programmable gate arrays," Springer, 2007.
- [18] Y. Zhu, and J. Weight "Ultrasonic nondestructive evaluation of highly scattering materials using adaptive filtering and detection," *IEEE Transaction on Ultrasonics, Ferroelectrics, and Frequency Control*, vol. 41, pp. 26–33, January 1994.
- [19] F. Tong, X. Xu, S. K. Tso, and B. L. Luk, "Identification of overlapped ultrasonic NDE echoes with adaptive deconvolution," *IEEE Proceedings of Mechatronics and Machines Vision in Practice*, pp. 48-51, 2007.
- [20] T. Wang, J. Saniie, and X. Jin "Analysis of low-order autoregressive models for ultrasonic grain signal characterization," *IEEE Transaction on Ultrasonics, Ferroelectrics, and Frequency Control*, vol. 38, pp. 116–124, March 1991.
- [21] D. Monroe, I. S. Ahn, and Y. Lu, "Adaptive filtering and target detection for ultrasonic backscattered signal," *IEEE International Conference on Electro/Information Technology*, pp. 1 – 6, May 2010.